

Superscatterer: Enhancement of scattering with complementary media

Tao Yang, Huanyang Chen, Xudong Luo,* and Hongru Ma
*Institute of Theoretical Physics, Shanghai Jiao Tong University,
Shanghai 200240, People's Republic of China*

(Dated: November 12, 2021)

Abstract

Based on the concept of complementary media, we propose a novel design which can enhance the electromagnetic wave scattering cross section of an object so that it looks like a scatterer bigger than the scale of the device. Such a “superscatterer” is realized by coating a negative refractive material shell on a perfect electrical conductor cylinder. The scattering field is analytically obtained by Mie scattering theory, and confirmed by full-wave simulations numerically. Such a device can be regarded as a cylindrical concave mirror for all angles.

PACS numbers: 41.20.Jb, 42.25.Fx

Recently great progress has been made [1, 2, 3, 4, 5, 6, 7, 8, 9, 10, 11, 12, 13] in manipulating the electromagnetic (EM) fields by means of metamaterials. By employing the coordinate transformation approach proposed by Leonhardt [1] and Pendry *et al.* [2], various exciting functional EM devices have been reported [4, 9, 10]. This methodology provides a clear geometric picture of those designed devices, and the permittivity and permeability tensors of designed functional materials can be derived from coordinate transformations directly. On the other hand, Mie scattering theory [11, 12, 14] provided an analytic approach to quantitatively analyze the scattering properties of EM fields, and the aforementioned functional devices can also be realized by choosing different scalar transformation functions. The combination of the geometric and the analytic approaches may give novel and surprising results. For example, in contrast to invisibility cloak, we may design an EM transformation media device to enlarge the scattering cross-section of a small object. In this way the object is effectively magnified to a size larger than the object plus the device so that it is much easier for EM wave detection, which we refer hereafter as a superscatterer.

In this Letter, we propose a generalized technique to achieve such a superscatterer. In the quasistatic limit, Nicorovici *et al.* [15] had demonstrated that the properties of a coated core can be extended beyond the shell into the matrix. It is called a *partially-resonant* system in which at least one dielectric constant of three-phase composite structure is negative. Moreover, by using the negative refracting material (NRM) [16, 17], Pendry and Ramakrishna [18] showed how to image an object by perfect cylindrical lens based on the concept of complementary media. Here we limit our discussion on the 2D case and prove that a special magnified image acts as a real object for EM wave detection.

Figure 1 shows a heuristic model stemmed from the concept of complementary media [18]. In Fig. 1(a), a slab of metamaterial with $\epsilon = \mu = -1$ images point source S at F_2 inside and F_1 outside the metamaterial if the distance between source and slab is less than the slab thickness. Now a perfect electrical conductor (PEC) boundary is set at R_1 , so the light propagating in the slab is completely reflected by it and focuses at I_2 inside and I_1 outside the slab. Since the slab and the vacuum with the same thickness are complementary to each other, it looks as if the medium between R_3 and R_1 is moved, and the PEC at R_1 is virtually shifted to R_3 and takes effect as a real PEC boundary. The picture can be extended to the 2D case as shown in Fig. 1(b), in which z axis is perpendicular to the paper. In the 2D case, the R_1 , R_2 and R_3 represent the radius of the inner region, the outer radius of

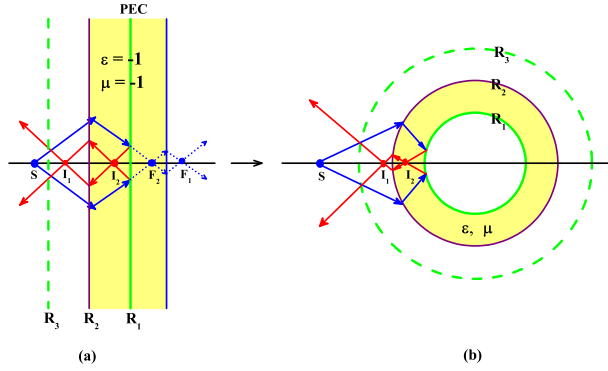


FIG. 1: (a) The schematic demonstration of the behavior of a beam propagates in a complementary media and PEC boundary. (b) The behavior is extended to the 2D case, where a superscatterer is formed with its effective size shown by the dashed line.

the cylindrical annulus (metamaterial shell) and the effective radius of the virtual cylinder, respectively. In order to move effectively the inner PEC boundary at $r = R_1$ to the surface of the virtual cylinder, where the radius is $r = R_3 > R_2$, both permittivity and permeability tensors in the metamaterial shell should be selected properly. The Mie scattering theory is a powerful tool to accomplish the goal.

We consider a transverse-electric (TE) polarized EM incident field with harmonic time dependence $\exp(-i\omega t)$. The coordinate system is the cylindrical coordinate coinciding with the cylinder we considered. In this coordinate system the permittivity and permeability tensors can be put in the following general form

$$\bar{\epsilon} = \epsilon_r(r)\hat{r}\hat{r} + \epsilon_\theta(r)\hat{\theta}\hat{\theta} + \epsilon_z(r)\hat{z}\hat{z}, \quad \bar{\mu} = \mu_r(r)\hat{r}\hat{r} + \mu_\theta(r)\hat{\theta}\hat{\theta} + \mu_z(r)\hat{z}\hat{z}. \quad (1)$$

The EM fields in the homogeneous material region ($r > R_2$) are well known and can be expressed by the superposition of cylindrical functions. The wave equation of E_z in the shell is written as

$$\frac{1}{\epsilon_z} \frac{1}{r} \frac{\partial}{\partial r} \left(\frac{r}{\mu_\theta} \frac{\partial E_z}{\partial r} \right) + \frac{1}{\epsilon_z} \frac{1}{r^2} \frac{\partial}{\partial \theta} \left(\frac{1}{\mu_r} \frac{\partial E_z}{\partial \theta} \right) + k_0^2 E_z = 0, \quad (2)$$

where k_0 is the wave vector of the EM wave in vacuum. Now we introduce a new coordinate system $(f(r), \theta, z)$, in which $f(r)$ is a continuous and piecewise differentiable function of the original radial coordinate r , the wave equation of field $\tilde{E}_z(f(r), \theta) = E_z(r, \theta)$ is transformed

to

$$\frac{1}{\epsilon_z} \frac{1}{r} f' \frac{\partial}{\partial f} \left(\frac{r}{\mu_\theta} f' \frac{\partial \tilde{E}_z}{\partial f} \right) + \frac{1}{\epsilon_z} \frac{1}{r^2} \frac{\partial}{\partial \theta} \left(\frac{1}{\mu_r} \frac{\partial \tilde{E}_z}{\partial \theta} \right) + k_0^2 \tilde{E}_z = 0, \quad (3)$$

where $f'(r)$ denotes $df(r)/dr$. By taking the components of permittivity and permeability tensors as [14],

$$\begin{aligned} \frac{\epsilon_r}{\epsilon_0} &= \frac{\mu_r}{\mu_0} = \frac{f(r)}{r} \frac{1}{f'(r)}, \\ \frac{\epsilon_\theta}{\epsilon_0} &= \frac{\mu_\theta}{\mu_0} = \frac{r}{f(r)} f'(r), \\ \frac{\epsilon_z}{\epsilon_0} &= \frac{\mu_z}{\mu_0} = \frac{f(r)}{r} f'(r), \end{aligned} \quad (4)$$

where ϵ_0 and μ_0 are the vacuum permittivity and permeability, the Eq. (3) can be solved by separation of variables $\tilde{E}_z = R(f)\Theta(\theta)$. The solution of $R(f)$ and $\Theta(\theta)$ are just the m th-order Bessel functions and $\exp(im\theta)$, in which m are integers.

With the above analysis, the electric fields in each domain are expressed as

$$E_z(r, \theta) = \begin{cases} 0, & r < R_1, \\ \sum_m \left(\alpha_m^i J_m(k_0 f(r)) + \alpha_m^s H_m^{(1)}(k_0 f(r)) \right) \exp(im\theta), & R_1 < r < R_2, \\ \sum_m \left(\beta_m^i J_m(k_0 r) + \beta_m^s H_m^{(1)}(k_0 r) \right) \exp(im\theta), & r > R_2. \end{cases} \quad (5)$$

where J_m and $H_m^{(1)}$ are the m th-order Bessel function and Hankel function of the first kind, respectively. By means of the orthogonality of $\exp(im\theta)$ and the continuity of E_z and H_θ at two interfaces ($r = R_1$ and $r = R_2$), we obtain the linear relationships between the coefficients as follows,

$$\alpha_m^i J_m(k_0 f(R_1)) + \alpha_m^s H_m^{(1)}(k_0 f(R_1)) = 0, \quad (6a)$$

$$\alpha_m^i J_m(k_0 f(R_2)) + \alpha_m^s H_m^{(1)}(k_0 f(R_2)) = \beta_m^i J_m(k_0 R_2) + \beta_m^s H_m^{(1)}(k_0 R_2), \quad (6b)$$

$$\frac{R_2}{f(R_2)} \left[\alpha_m^i J_m'(k_0 f(R_2)) + \alpha_m^s H_m^{(1)'}(k_0 f(R_2)) \right] = \beta_m^i J_m'(k_0 R_2) + \beta_m^s H_m^{(1)'}(k_0 R_2), \quad (6c)$$

where the prime denotes differentiation with respect to the entire argument of Bessel functions. By imposing the boundary condition of $f(r)$, $f(R_2) = R_2$, we get the solutions of Eqs.(6) as follows,

$$\frac{\alpha_m^s}{\alpha_m^i} = \frac{\beta_m^s}{\beta_m^i} = -\frac{J_m(k_0 f(R_1))}{H_m^{(1)}(k_0 f(R_1))}, \quad m = 0, \pm 1, \pm 2, \dots \quad (7)$$

This is the exact solution for scattering matrix.

We can draw some interesting conclusions from Eqs. (7). If $f(r)$ is a monotonic function and $f(R_1) = R_3 > R_2$, the material of the shell must be NRM from Eqs.(4), and the fields at point (r, θ, z) in inner annulus $R_1 < r < R_2$ are equal to those at point $(f(r), \theta, z)$ in outer region $R_2 < r < R_3$. Moreover, in the region $r > R_3$, the scattering fields are exactly equal to those scattered by a PEC cylinder with radius R_3 , as if whole cylindrical annulus of $R_1 < r < R_3$ is moved and the PEC boundary at $r = R_1$ is magnified and shifted to $r = R_3$. Here, the cylinder with radius $f(R_1)$ is called a virtual cylinder. It is just the expected result in Fig. 1(b).

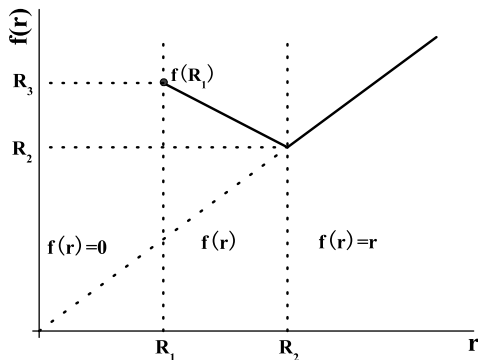


FIG. 2: A simple function $f(r)$ satisfies the condition of Fig.1(b)

For simplicity, we choose a linear function for $f(r)$,

$$f(r) = \begin{cases} b_0(R_2 - r)/(R_2 - R_1) + R_2, & R_1 < r < R_2, \\ r, & r > R_2. \end{cases} \quad (8)$$

Here b_0 is an important parameter to determine the magnification factor. It should be noted that both cloak and concentrator can also be obtained in the same manner. For example, it is a perfect cloak when $b_0 = -R_2$, and it becomes an imperfect cloak when $R_1 - R_2 > b_0 > -R_2$, or a concentrator when $b_0 > R_1 - R_2$ and $f(r) = rf(R_1)/R_1$ in the region $r < R_1$. However, the case $b_0 > 0$, which provides a folded geometry [19, 20], is less discussed. In fact, with the help of the geometric picture of the concentrator, it means a big cylinder with radius $b_0 + R_2$ is compressed into a small cylinder with radius R_1 , and the gap between $r = R_1$ and $r = b_0 + R_2$ has to be filled by a pair of complementary media: One is the vacuum in $R_2 < r < b_0 + R_2$ and the other is the NRM shell in $R_1 < r < R_2$.

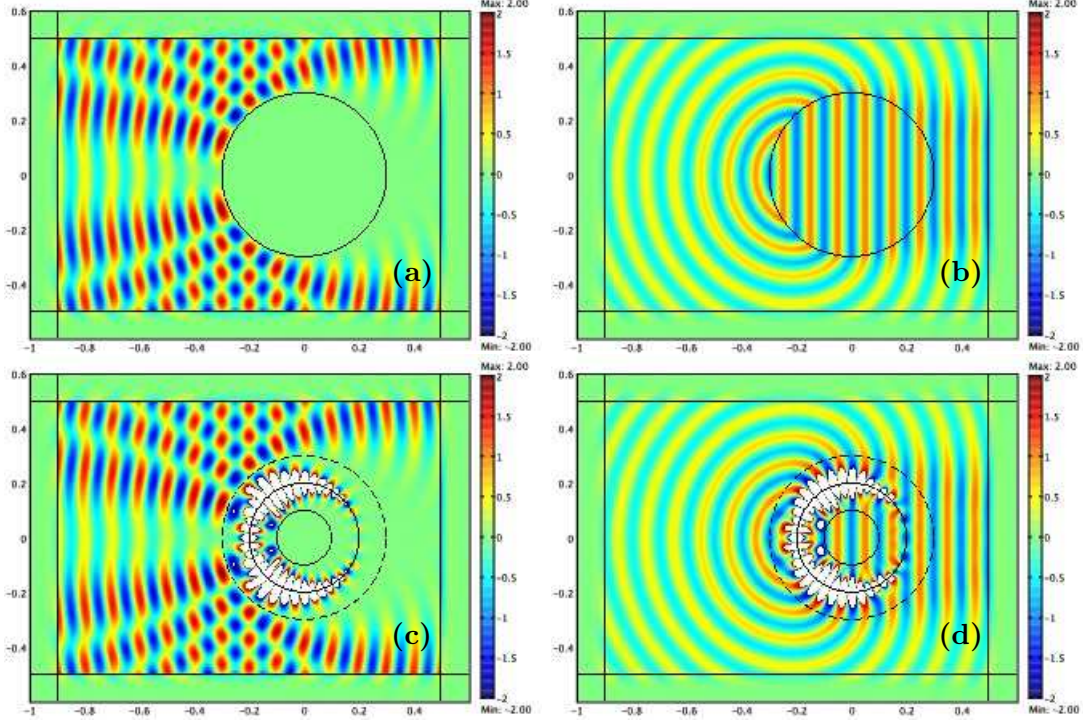


FIG. 3: Snapshot of the total and scattering electric field. (a) - (b) The total and scattering electric fields induced by PEC cylinder with radius $R_3 = 0.3\text{m}$, respectively. (c) - (d) The total and scattering electric fields induced by the designed device (the radius of virtual cylinder is 0.3m), respectively.

This device scatters the same fields as the uncompressed cylinder, which extends beyond the shell, so we call it “superscatterer”.

Next, we present the patterns of electric field calculated by finite element solver of the Comsol Multiphysics software package. In Fig. 3, the plane wave is normal incident from left to right with frequency 3 GHz and unit amplitude, and the inner and outer radii of the shell are $R_1 = 0.1\text{m}$ and $R_2 = 0.2\text{m}$, respectively. When b_0 is equal to 0.1m and the function $f(r)$ is taken as in Eq. (8), the radius of the virtual cylinder becomes $f(R_1) = b_0 + R_2 = 0.3\text{m}$. The ranges of the components of $\bar{\epsilon}$ and $\bar{\mu}$ are taken as follows: $\epsilon_r, \mu_r \in [-3, -1]$, $\epsilon_\theta, \mu_\theta \in [-1, -\frac{1}{3}]$, and $\epsilon_z, \mu_z \in [-3, -1]$. A tiny absorptive imaginary part ($\sim 10^{-5}$) is added to $\bar{\epsilon}$ and $\bar{\mu}$ due to the inevitable losses of the NRM.

Fig. 3(a) and 3(b) are snapshots of the total electric field and scattering electric field induced by a PEC cylinder with radius $R_3 = 0.3\text{m}$, respectively; Fig. 3(c) and 3(d) are those fields induced by the superscatterer. Comparing the patterns of electric field in the

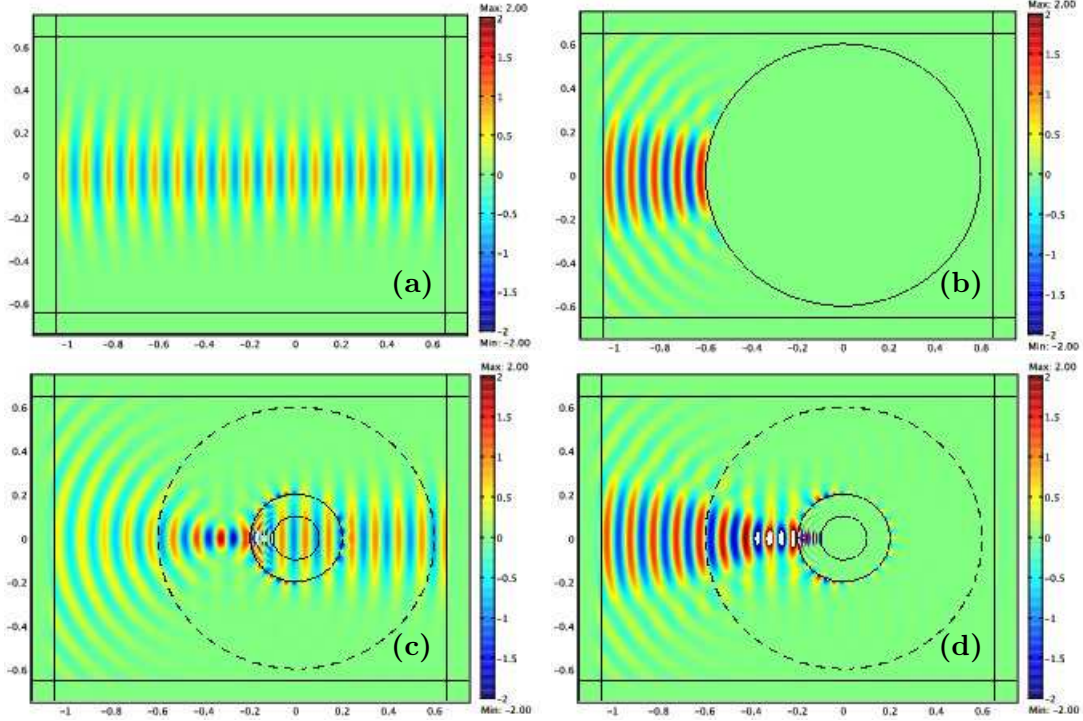


FIG. 4: (a) A Gaussian beam in free space. (b) The total electric field induced by PEC cylinder with radius 0.6m. (c) - (d) The scattering and total fields by the superscatterer (the radius of the virtual cylinder is 0.6m), respectively.

region $r > R_3$, one can find they are almost equivalent. Here, the bounds of the amplitude of electric field in Fig. 3 set from -2 to 2 for clarity. The white flecks in the region of the complementary media show the regions where the values of fields exceed the bounds. The highest value of the field in the flecks is about 10^2 , which comes from the dominative high- m modes with the factor $J_m(k_0 R_3) H_m^{(1)}(k_0 f(r)) / H_m^{(1)}(k_0 R_3)$ in the scattering field.

We define the magnification factor η as $f(R_1)/R_2$, which is the ratio of the radius of the virtual cylinder to the real size of this device. The components of permittivity and permeability tensors are negative for the case of $\eta > 1$. There is no singularity for any finite η as long as both $f(r)$ and $f'(r)$ are nonzero in $R_1 \leq r \leq R_2$. For example, when $\eta = 20$, the ranges of the parameters are: $\epsilon_r, \mu_r \in [-1.1, -0.052]$, $\epsilon_\theta, \mu_\theta \in [-19, -0.90]$, and $\epsilon_z, \mu_z \in [-399, -19]$.

Moreover, the device in Fig. 1(b) can be regarded as a cylindrical concave mirror for all angles, which can not be realized by ordinary media. From the theory of geometrical optics, when a plane wave incidents on it, the paraxial beams focus at $r = f(R_1)/2 = (b_0 + R_2)/2$.

Here, a full-wave simulations with COMSOL Multiphysics are used to test the focus behavior of a Gaussian beam propagated from left to right with unit amplitude. Fig. 4(a)-(d) give the snapshots of the Gaussian beam in free space, the total electric field induced by PEC cylinder with radius 0.6m, and the scattering and total electric fields induced by the superscatterer (here $R_1 = 0.1\text{m}$, $R_2 = 0.2\text{m}$ and $b_0 = 0.4\text{m}$), respectively. The scattering electric field in Fig. 4(c) shows the focus is approximately at $r = 0.3\text{m}$ since Gaussian beam is close to a paraxial beam. Here, it is worthy noting that the superscatterer becomes a cylindrical concave mirror for all angles if and only if there is $b_0 > R_2$. In principle, if we make the radius $f(R_1)$ of virtual cylinder to infinity by adjusting the function $f(r)$, the cylindrical concave mirror becomes a plane mirror for all angles, so that any parallel light incidents to the superscatterer will be reflected straight back along the incident path.

In conclusion, we demonstrated the properties of a “superscatterer” in terms of PEC boundary and properly complementary media. This kind of functional devices might be important in EM detection. Similar concept can be extended to the case of non PEC boundary and three dimension.

The work is supported by the National Natural Science Foundation of China under grant No.10334020 and in part by the National Minister of Education Program for Changjiang Scholars and Innovative Research Team in University.

* To whom correspondence should be addressed.

Email address: luoxd@sjtu.edu.cn

- [1] U. Leonhardt, *Science* **312**, 1777 (2006).
- [2] J. B. Pendry, D. Schurig, and D. R. Smith, *Science* **312**, 1780 (2006).
- [3] A. Greenleaf, M. Lassas, and G. Uhlmann, *Physiol. Meas.* **24**, 413 (2003).
- [4] D. Schurig, J. J. Mock, B.J. Justice, S. A. Cummer, J. B. Pendry, A. F. Starr, and D. R. Smith, *Science* **314**, 977 (2006).
- [5] A. Alù and N. Engheta, *Phys. Rev. E* **72**, 016623 (2005).
- [6] S. A. Cummer, B.-I. Popa, D. Schurig, D. R. Smith, and J. B. Pendry, *Phys. Rev. E* **74**, 036621 (2006).
- [7] Z. Jacob, L. A. Alekseyev, and E. Narimanov, *Opt. Express* **14**, 8247 (2006).

- [8] W. Cai, U. K. Chettiar, A. V. Kildishev, and V. M. Shalaev, *Nat. Photon.* **1**, 224 (2007).
- [9] M. Rahm, D. Schurig, D. A. Roberts, S. A. Cummer, D. R. Smith, and J. B. Pendry, *Photon. Nanostruct.: Fundam. Applic.* **6**, 87 (2008).
- [10] H. Y. Chen and C. T. Chan, *Appl. Phys. Lett.* **90**, 241105 (2007).
- [11] H. Chen, B.-I. Wu, B. Zhang, and J. A. Kong, *Phys. Rev. Lett.* **99**, 063903 (2007).
- [12] Z. Ruan, M. Yan, C.W. Neff, and M. Qiu, *Phys. Rev. Lett.* **99**, 113903 (2007).
- [13] X. H. Zhang, H. Y. Chen, X. D. Luo, and H. R. Ma, *Opt. Express* **16**, 11764 (2008).
- [14] A.D.Yaghjian and S.Maci, arXiv:0710.2933.
- [15] N. A. Nicorovici, R. C. McPhedran, and G. W. Milton, *Phys. Rev. B* **49**, 8479 (1994); G. W. Milton, N. A. Nicorovici, R. C. McPhedran and V. A. Podolskiy, *Proc. R. Soc. London, Ser. A* **461**, 3999 (2005).
- [16] V. G. Veselago, *Sov. Phys. Usp.* **10**, 509 (1968).
- [17] J. B. Pendry, *Phys. Rev. Lett.* **85**, 3966 (2000).
- [18] J. B. Pendry and S. A. Ramakrishna, *J. Phys.: Condens. Matter* **14**, 8463 (2002); **15**, 6345 (2003).
- [19] U. Leonhardt and T. G. Philbin, *New J. Phys.* **8**, 247 (2006).
- [20] G. W. Milton, N. P. Nicorovici, R. C. McPhedran, K. Cherednichenko, and Z. Jacob, arXiv:0804.3903.